Supporting Information

Observation of complete pressure-jump protein refolding in molecular dynamics simulation and experiment

Yanxin Liu,[†], Maxim B. Prigozhin,[§] Klaus Schulten,[*,§,†,‡] and Martin Gruebele[*,§,†,‡]

[†] Department of Physics, Center for the Physics of Living Cells, and Beckman Institute,
[§] Department of Chemistry, [‡] Center for biophysics and computational biophysics, University of Illinois, Urbana, Illinois 61801, United States

[*]email: mgruebel@illinois.edu or kschulte@ks.uiuc.edu

Movies

- **Movie S1** shows the trajectory of the unfolding simulation. The crystal structure was used as the initial state. The pressure was increased gradually from 1 bar to 5 kbar in $0.15\,\mu$s at a rate of $1\,\text{bar}/30\,\text{ps}$ while maintaining the temperature at $T = 325\,\text{K}$. For the next $0.15\,\mu$s, the temperature was increased to $525\,\text{K}$ while maintaining the pressure at $P = 5\,\text{kbar}$. After the protein completely unfolded, the temperature was dropped back to $325\,\text{K}$, but the pressure was kept at $P = 5\,\text{kbar}$. The denatured protein was equilibrated for $1\,\mu$s at high pressure. The pressure was then dropped gradually from 5 kbar to 1 bar in $0.15\,\mu$s at a rate of $-1\,\text{bar}/30\,\text{ps}$ while maintaining the temperature at $T = 325\,\text{K}$.

- **Movie S2** shows the 32-μs refolding trajectory from the simulation at $T = 325\,\text{K}$ and $P = 1\,\text{bar}$ after pressure drop.

- **Movie S3** shows the refolding trajectory in the time window between $18\,\mu$s and $20\,\mu$s. Sequential local folding events were observed in this time window. After helices 1 and 4 have aligned themselves correctly relative to the crystal structure, helices 2 and 3 formed the native packing with helices 1 and 4, followed by the formation of loop 1 and then loop 3.

Methods

Protein expression and purification. Proteins were purified as described previously in Ref 35 cited in main text. Guanidine hydrochloride (>99%, GuHCl) and N-acetyl-tryptophanamide (NATA) were purchased from Sigma Inc. (St. Louis, MO) and used without further purification. Potassium phosphate was purchased from EMD Chemicals (Billerica, MA). Protein samples were used in 50 mM potassium phosphate buffer at pH = 7.1 unless otherwise noted.

Fluorescence thermodynamics under pressure. Pressure titration was done using a commercial pressurization cell from ISS (Champaign, IL). $\sim$400 μL of 200 μM protein sample was placed in a rectangular quartz cuvette with path length of 4 mm. The cuvette was closed with a plastic cap and sealed with Teflon tape. The cuvette was then placed into the pressurization cell and the system was pressurized by pumping spectrophotometric grade ethyl alcohol (95% A. C. S. reagent from Acros Organics, Geel, Belgium) into the cell with a high-pressure pump (High Pressure Equipment Company, Erie, PA). Fluorescence spectra were collected using a Cary Eclipse fluorescence spectrophotometer (Varian, Palo Alto, CA). The sample was excited at 280 nm and fluorescence was collected from 290 to 545 nm with a scan rate of 120 nm/min. The width of both excitation and emission slits was 5 nm. The center of spectral mass reported in Figure S4 was calculated as the weighted average of the fluorescence intensity: $<l> = \int d\lambda \lambda l(\lambda) / \int d\lambda l(\lambda)$.

Results

Equilibrium pressure denaturation monitored by fluorescence. We investigated equilibrium pressure denaturation of λ*YG using fluorescence spectroscopy. Figure S4A shows fluorescence spectra of λ*YG in 1 M GuHCl in the pressure range from 1 to 2.5 kbar. Figure S4B shows the shifts of the center of spectral mass for the tryptophan derivative N-acetyl-tryptophanamide (NATA), λ*YG in 50 mM phosphate buffer, and λ*YG in 1 M GuHCl. NATA and λ*YG in buffer have very similar spectral mass shift, which suggests that this shift arises mostly due to the intrinsic sensitivity of tryptophan fluorescence to hydrostatic pressure. However, λ*YG in 1 M GuHCl shows a significantly larger spectral shift as compared to that of NATA or λ*YG in buffer, which indicates the pressure-induced unfolding of λ*YG, similar to the λ*YA mutant.
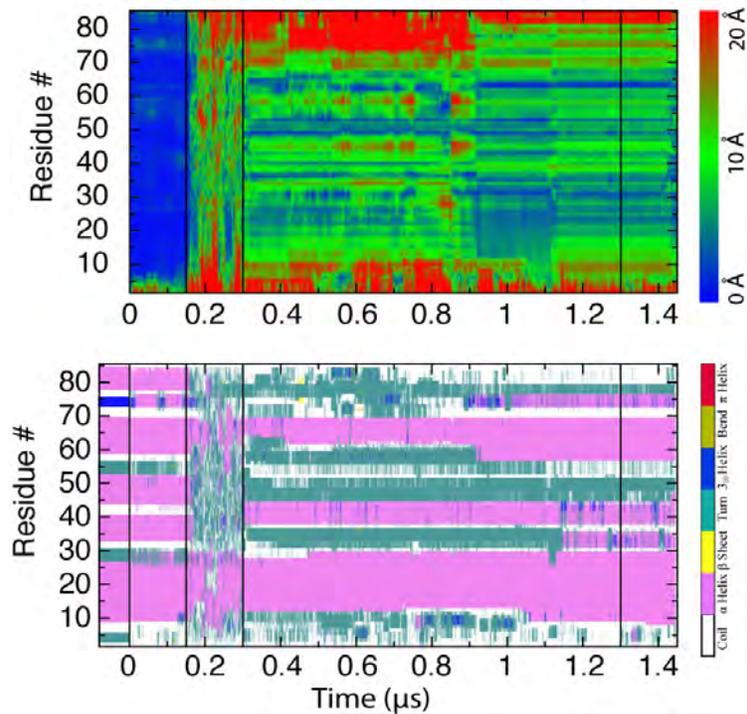
Figures

Figure S1: Structural characterization of the λ*YG unfolding trajectory from simulation. (Top) Time evolution of per residue C$_\alpha$ displacement from the crystal structure. (Bottom) Time evolution of the secondary structure per residue. The secondary structure of the crystal structure is shown at left.
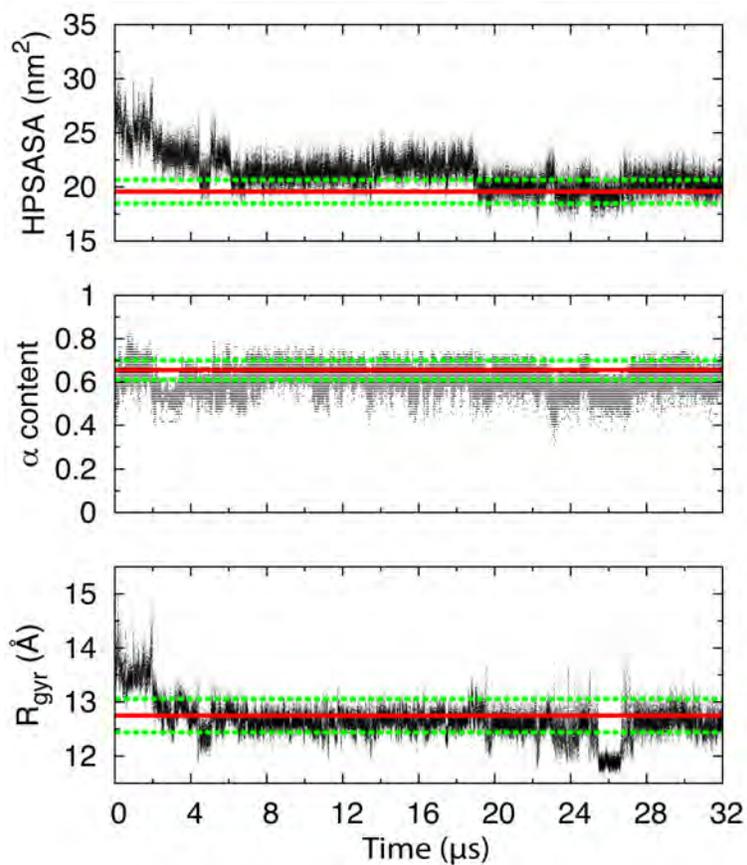
Figure S2: The protein refolding trajectory from the simulation at $T = 325\,\mathrm{K}$ and $P = 1\,\mathrm{bar}$ after pressure drop. HPSASA refers to the solvent accessible surface area (SASA) of hydrophobic groups. α-content is the fraction of residues that are in the α-helical conformation. R_{gyr} is the radius of gyration. The native range is defined by the mean value (red solid line) $\pm$ standard deviation (green dashed line) from a 0.3-μs equilibrium simulations of the native structure at $T = 325\,\mathrm{K}$ and $P = 1\,\mathrm{bar}$.
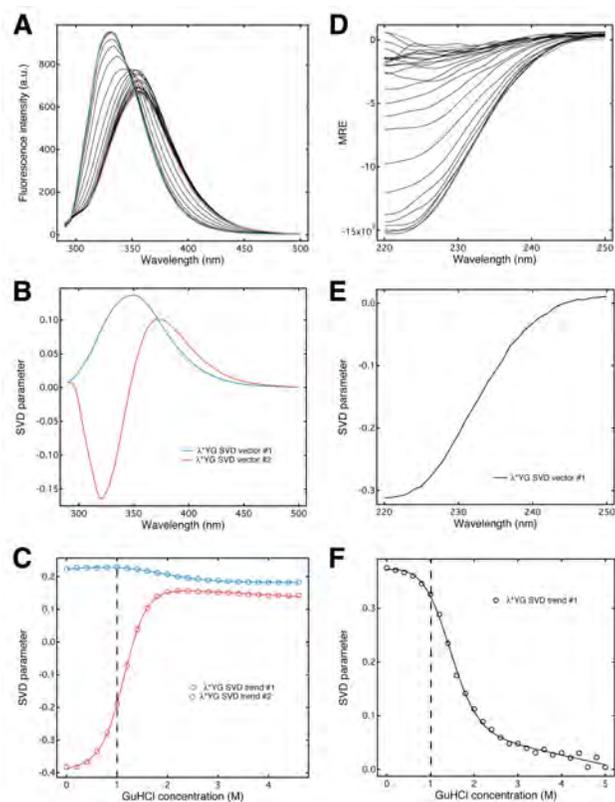
Figure S3: Titration of λ*YG with GuHCl monitored by fluorescence spectroscopy (A-C) and circular dichroism spectroscopy (D-F). (A, D) The spectra were collected from 0 M GuHCl (green) to 4.8 M GuHCl (magenta). The spectra were smoothed with 3-point binomial smoothing (B, E) Basis vectors from singular value decomposition of the spectra in A and D, respectively. (C, F) Basis vector trends (circles) and the corresponding two-state thermodynamic fits (lines). The onset of a transition at 1M GuHCl is highlighted with vertical dashed lines.
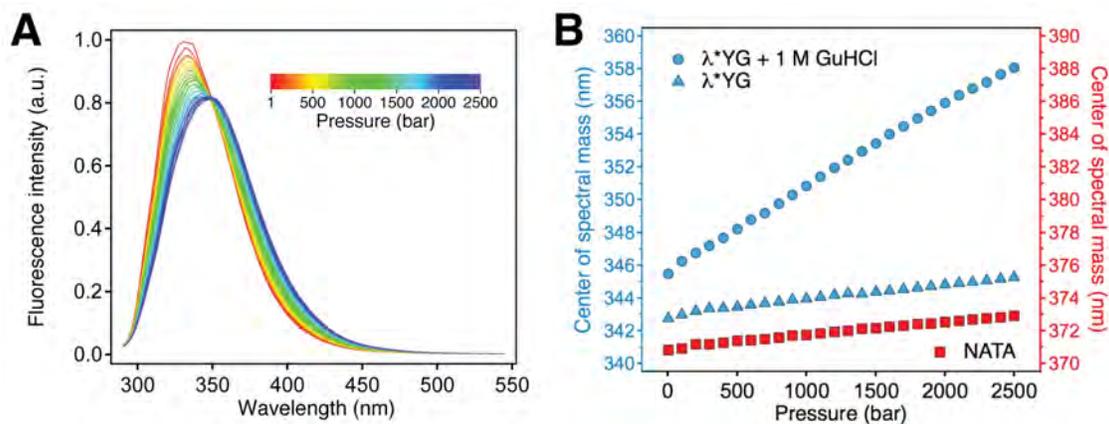
Figure S4: Equilibrium pressure denaturation of λ*YG probed by fluorescence spectroscopy. (A) Fluorescence spectra of λ*YG in 1 M GuHCl taken in the intervals of 100 bar from 1 bar to 2.5 kbar. (B) Center of spectral mass for NATA and λ*YG in buffer shifts to a much lesser extent than λ*YG in 1 M GuHCl, which suggests that the protein is unfolding in the latter case.
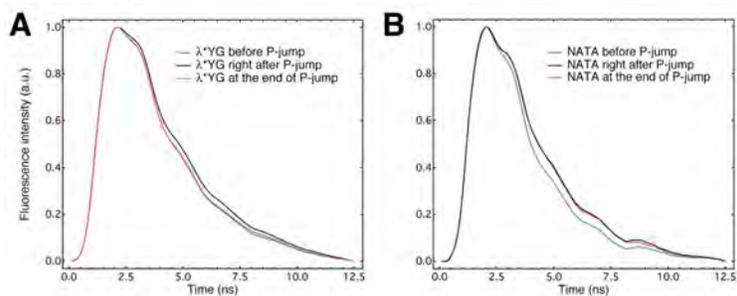
Figure S5: Fluorescence decays of λ*YG (A) and NATA (B) before the pressure jump (P=1.2 kbar, blue trace), right after the pressure jump (P=1 bar, black trace), and 5 ms after the jump (P=1 bar, red trace). Each trace is an average of 100 individual traces.
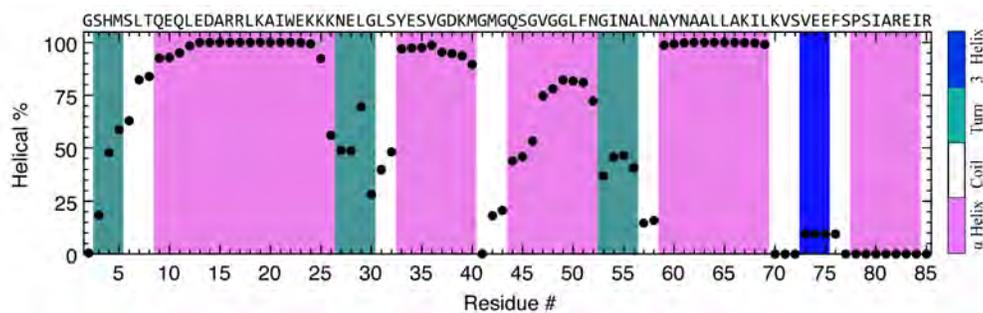
Figure S6: Residue-specic α-helical propensity calculated from the refolding simulation. The helical percentage was defined as the time percentage each residue spent in α-helical conformation during the last $30\,\mu$s of refolding simulation. The secondary structure of the crystal structure is shown as a color-coded background, and the sequence at the top.
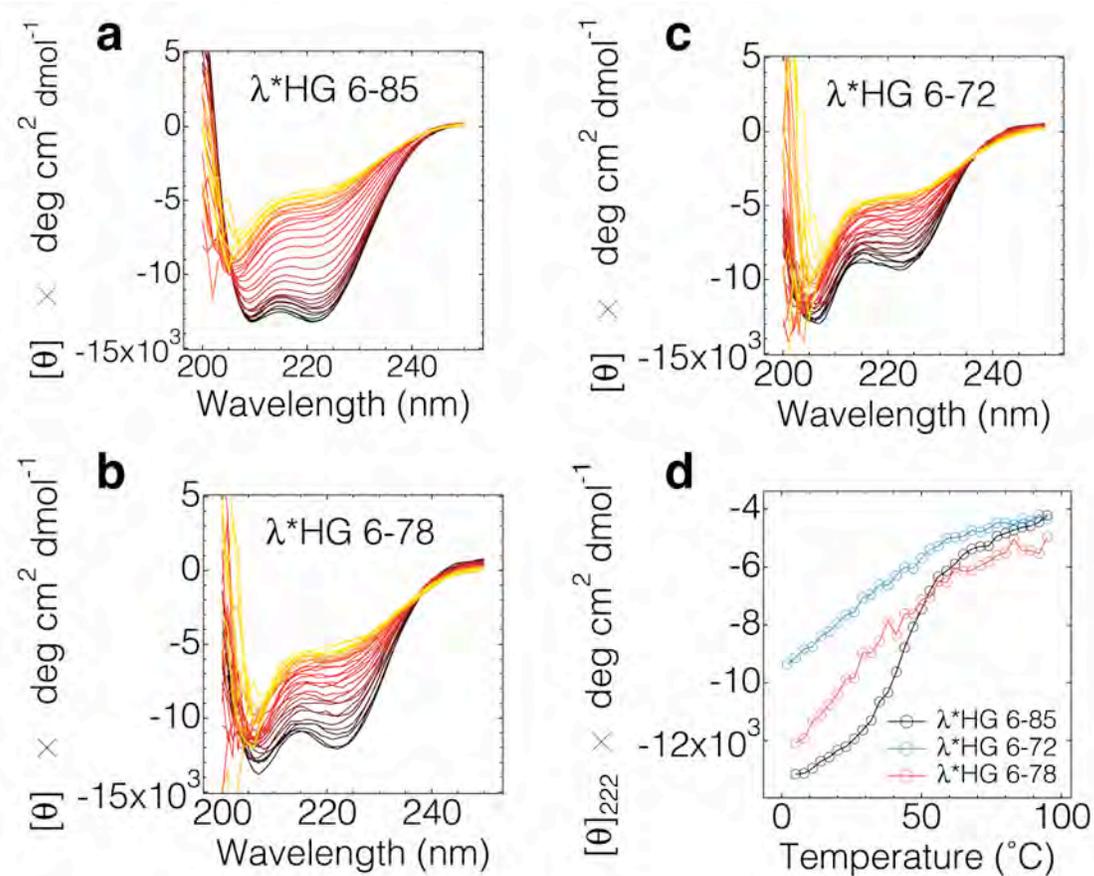
FIGURE S7: (a) – (c) Circular dichroism spectra of a lambda repressor fragment and two C-terminal truncations. (d) Thermal melt of the truncations is less cooperative than the melt of the native state.
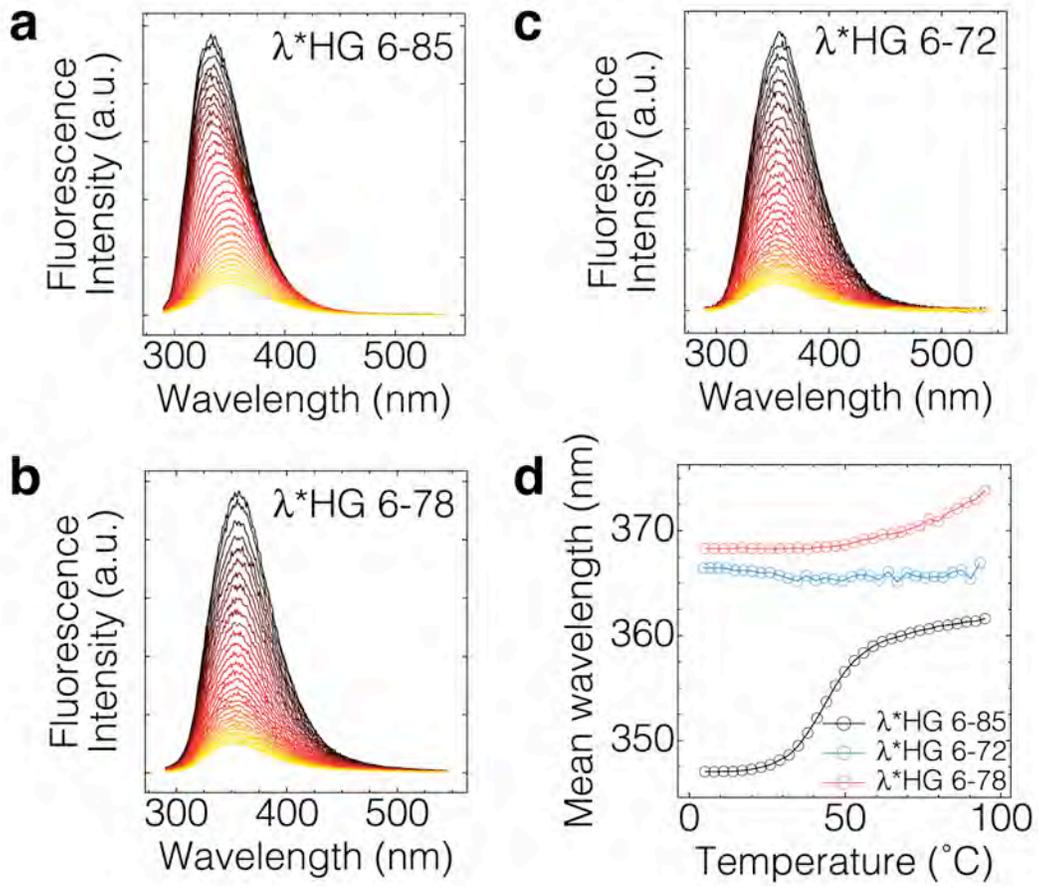
FIGURE S8: (a) – (c) Tryptophan fluorescence spectra of a lambda repressor fragment and two C-terminal truncations. (d) Thermal melt of the truncations is less cooperative than the melt of the native state.